Current bounds and future prospects of light neutralino dark matter in the NMSSM

Rahool Kumar Barman, Indian Association for the Cultivation of Science

based on arXiv: 2006.07854

(with Genevieve Belanger (LAPTh), Biplob Bhattacherjee (IISc), Rohini Godbole (IISc), Dipan Sengupta (Univ. of California), Xerxes Tata (Univ. of Hawaii))

Snowmass EF10 DM@colliders, Topical meeting on benchmark for WIMPs

July 2, 2020

Why NMSSM?

1. The next-to-Minimal Supersymmetric Standard Model (NMSSM) offers an elegant solution to the μ-problem in MSSM through the introduction of an additional singlet superfield ($\hat{S}$).

$$W_{MSSM} = y_u^{ij}\hat{u}_i\hat{Q}_j \cdot \hat{H}_u - y_d^{ij}\hat{d}_i\hat{Q}_j \cdot \hat{H}_d - y_e^{ij}\hat{E}_i\hat{L}_j \cdot \hat{H}_d + \boxed{\mu\hat{H}_u \cdot \hat{H}_d}$$

$$W_{NMSSM} = W_{MSSM}(\mu = 0) + \lambda\hat{S}\hat{H}_u \cdot \hat{H}_d + \frac{k}{3}\hat{S}^3$$

2. The NMSSM naturally generates an effective μ term when S develops a non-zero vev $< S >$. λ and κ are dimensionless parameters.

Why NMSSM?

1. The next-to-Minimal Supersymmetric Standard Model (NMSSM) offers an elegant solution to the μ-problem in MSSM through the introduction of an additional singlet superfield ($\hat{S}$).

$$W_{MSSM} = y_u^{ij}\hat{u}_i\hat{Q}_j \cdot \hat{H}_u - y_d^{ij}\hat{d}_i\hat{Q}_j \cdot \hat{H}_d - y_e^{ij}\hat{E}_i\hat{L}_j \cdot \hat{H}_d + \boxed{\mu\hat{H}_u \cdot \hat{H}_d}$$

$$W_{NMSSM} = W_{MSSM}(\mu = 0) + \boxed{\lambda\hat{S}\hat{H}_u \cdot \hat{H}_d} + \frac{k}{3}\hat{S}^3$$

2. The NMSSM naturally generates an **effective μ term** ($\mu \sim \lambda < S >$) when S develops a non-zero vev $< S >$. λ and κ are dimensionless parameters.

Why NMSSM?

1. A phenomenologically richer Higgs sector compared to MSSM:
   7 Higgs bosons: 3 CP-even states (h_1, h_2 and h_3), 2 CP-odd states (a_1 and a_2) and 2 charged Higgses ($H^{\pm}$).
2. Offers an exciting possibility to have light singlet-dominated a_1 and/or h_1 below 125 GeV (Ref. [12, 11, 22, 21, 23, 16]).
3. The tree level Higgs sector is driven by:

$$\lambda,\ \kappa,\ A_\lambda,\ A_\kappa,\ \tan\beta,\ \mu$$

   A_λ and A_κ are the trilinear soft-breaking parameters.

Why NMSSM?

1. Compared to MSSM, the neutral electroweak ino sector also has an additional neutralino:

The neutralino mass matrix:

$$M_{\chi_i^0} = \begin{pmatrix} M_1 & 0 & -M_Z \sin\theta_W \cos\beta & M_Z \sin\theta_W \sin\beta & 0 \\ 0 & M_2 & M_Z \cos\theta_W \cos\beta & -M_Z \cos\theta_W \sin\beta & 0 \\ -M_Z \sin\theta_W \cos\beta & M_Z \cos\theta_W \cos\beta & 0 & -\mu & -\lambda v \sin\beta \\ M_Z \sin\theta_W \sin\beta & -M_Z \cos\theta_W \sin\beta & -\mu & 0 & -\lambda v \cos\beta \\ 0 & 0 & -\lambda v \sin\beta & -\lambda v \cos\beta & 2\kappa v_s \end{pmatrix}$$

Here, M_1: bino mass parameter, M_2: wino mass parameter, $\tan\beta$: ratio of vev of the Higgs doublets.

2. The charginos are composed of winos and higgsinos.
3. The neutralinos can be admixtures of *singlino*, bino, wino and higgsinos.
4. At the tree level, the EW ino sector is controlled by: $M_1,\ M_2,\ \mu, \tan\beta,\ \lambda, \kappa$

Why NMSSM?

- In the MSSM with heavy sfermions, light neutralinos below $\sim 30\ \mathrm{GeV}$ are constrained [18, 5, 15, 9, 8, 7, 17, 4].
- This arises mainly from a combination of the direct detection constraint, the relic density constraint and the chargino mass constraint.
- The NMSSM allows the possibility of a lighter neutralino ($\lesssim 30\ \mathrm{GeV}$) while satisfying the upper limit on the relic density and other current constraints (Ref. [2, 10, 1, 19, 13, 3, 14]).
- In such cases, the singlet-dominated light Higgses provide an efficient annihilation mechanism for these light neutralinos in the early universe [6, 20].

Outline of this work

- We assume a standard cosmological scenario, considering parameter space points with $\Omega h^2 \leq 0.120$ and focus on the $M_{\widetilde{\chi}_1^0} \leq 62.5$ GeV region that can potentially contribute to invisible decays of the SM-like Higgs boson.
- The parameter region thus obtained is subjected to current collider, cosmological and astrophysical constraints.
- The allowed parameter space is investigated along the following future directions:
  1. future multi-ton direct detection experiments.
  2. invisible Higgs decay width measurement at the future LHC, FCC, ILC and CEPC.
  3. direct light Higgs searches and direct electroweakino searches at the HL-LHC and the HE-LHC.

Parameter space

1. We choose the parameter space with h_1 and a_1 below 122 GeV.
2. h_2 is identified with the SM-like Higgs boson.

$$0.01 < \lambda < 0.7,\ 10^{-5} < \kappa < 0.05,\ 3 < \tan\beta < 40$$
$$100\ \text{GeV} < \mu < 1\ \text{TeV},\ 1.5\ \text{TeV} < M_3 < 10\ \text{TeV}$$
$$2\ \text{TeV} < A_\lambda < 10.5\ \text{TeV},\ -150\ \text{GeV} < A_\kappa < 100\ \text{GeV}$$
$$M_1 = 2\ \text{TeV},\ 70\ \text{GeV} < M_2 < 2\ \text{TeV}$$
$$A_t = 2\ \text{TeV},\ A_{b,\tilde{\tau}} = 0,\ M_{U_R^3}, M_{D_R^3}, M_{Q_L^3} = 2\ \text{TeV},\ M_{e_L^3}, M_{e_R^3} = 3\ \text{TeV}$$

The allowed parameter space

- The $\widetilde{\chi}_1^0$ has to be bino or singlino dominated.
- In such cases, $\Omega h^2 \leq 0.122$ can be satisfied only through co-annihilation or annihilation via resonance.
- For our parameter space, co-annihilation $\longrightarrow$ *not feasible*
- Only possibility $\rightarrow$ annihilation via resonance.
- We fix M_1 at 2 TeV $\rightarrow$ $\widetilde{\chi}_1^0$ is always singlino dominated.
- a_1 and h_1 is always singlet dominated.

- Below the Z funnel region:
  1. the allowed points are mostly populated along $M_{a_1} \sim 2M_{\widetilde{\chi}_1^0}$.
  2. points away from the above correlation have $M_{h_1} \sim 2M_{\widetilde{\chi}_1^0}$.

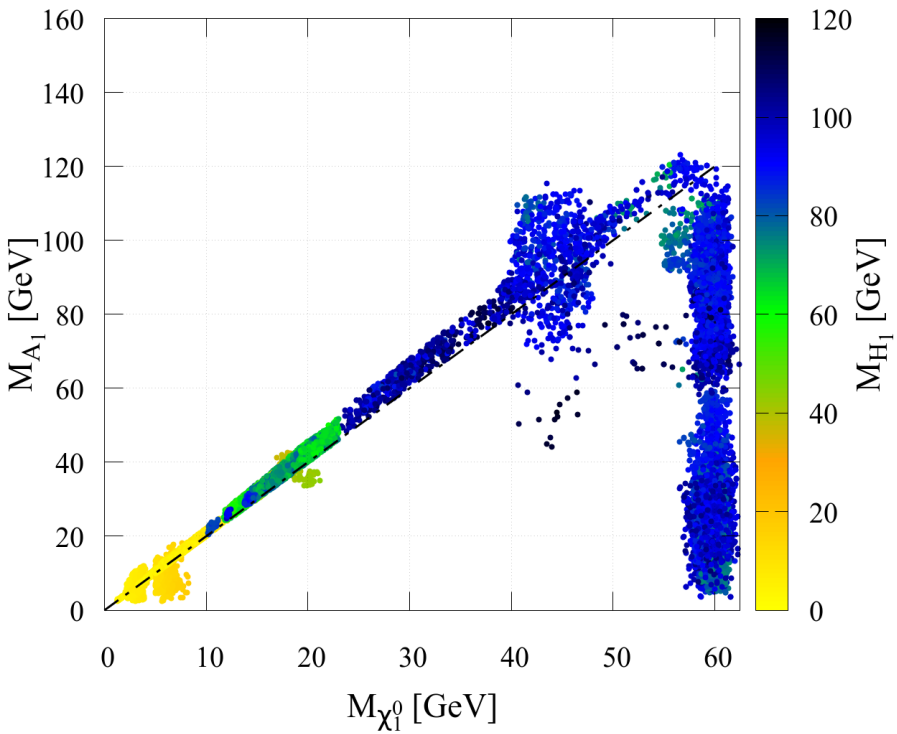

Higgs invisible measurement at future experiments

- Projected capability of future experiments to probe invisibly decaying Higgs boson:

  HL-LHC ($\gtrsim 2.8\%$) [CMS-PAS-FTR-16-002],
  FCC-ee ($\gtrsim 0.63\%$) [1605.00100],
  ILC ($\gtrsim 0.4\%$) [1310.0763],
  CEPC ($\gtrsim 0.24\%$) [1811.10545],
  FCC-hh ($\gtrsim 0.01\%$) [CERN-ACC-2018-045].

In the present case, multiple decay modes can potentially contribute to $Br(H_{125} \to invisible)$:

- $H_{125} \to \widetilde{\chi}_1^0 \widetilde{\chi}_1^0$
- $H_{125} \to A_1 A_1 \to 4\widetilde{\chi}_1^0$
- $H_{125} \to H_1 H_1 \to 4\widetilde{\chi}_1^0$
- $H_{125} \to \widetilde{\chi}_2^0 \widetilde{\chi}_1^0 \to (\widetilde{\chi}_2^0 \to H_1 \widetilde{\chi}_1^0)\widetilde{\chi}_1^0 \to (H_1 \to \widetilde{\chi}_1^0 \widetilde{\chi}_1^0) 2\widetilde{\chi}_1^0 \to 4\widetilde{\chi}_1^0$
- $H_{125} \to \widetilde{\chi}_2^0 \widetilde{\chi}_1^0 \to (\widetilde{\chi}_2^0 \to A_1 \widetilde{\chi}_1^0)\widetilde{\chi}_1^0 \to (A_1 \to \widetilde{\chi}_1^0 \widetilde{\chi}_1^0) 2\widetilde{\chi}_1^0 \to 4\widetilde{\chi}_1^0$

Complementarity between future direct detection and invisible Higgs measurements

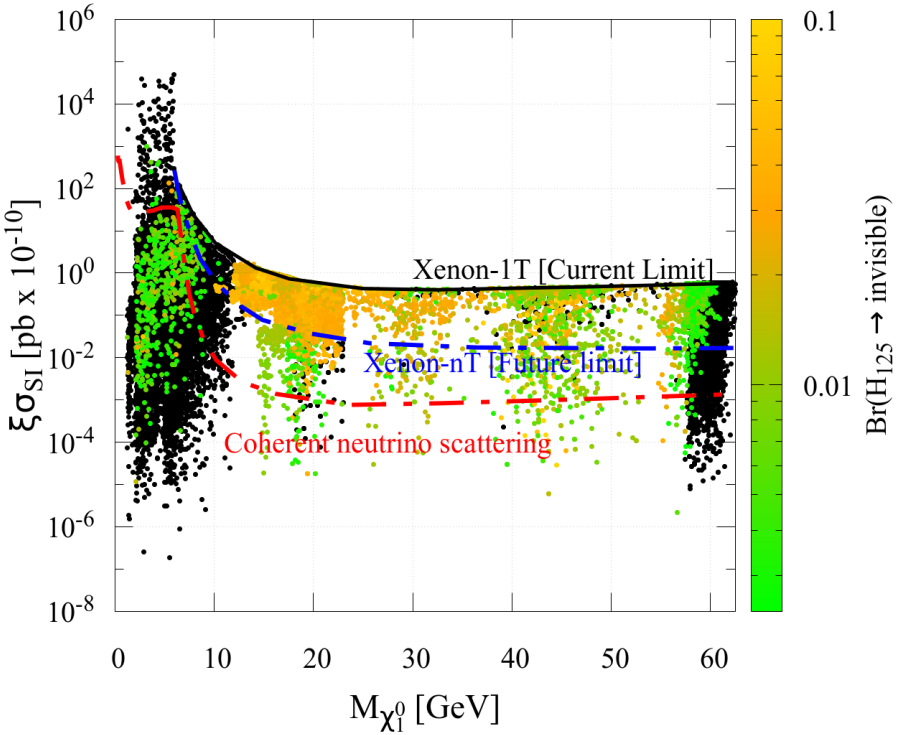

Here, ξ is $\Omega h^2/0.122$.

Black colored points

$Br(H_{125} \to invisible) < 0.24\% \to$ outside the projected Higgs invisible measurement capability of CEPC.

- CEPC will be able to probe the green colored points in the $M_{\tilde{\chi}_1^0} \lesssim$ 10 GeV region which may be forever outside the reach of DM detectors.
- CEPC will also be able to probe points which are outside Xenon-nT's future reach and which fall below the neutrino scattering floor, over the entire mass range.

Projected reach of future light Higgs searches

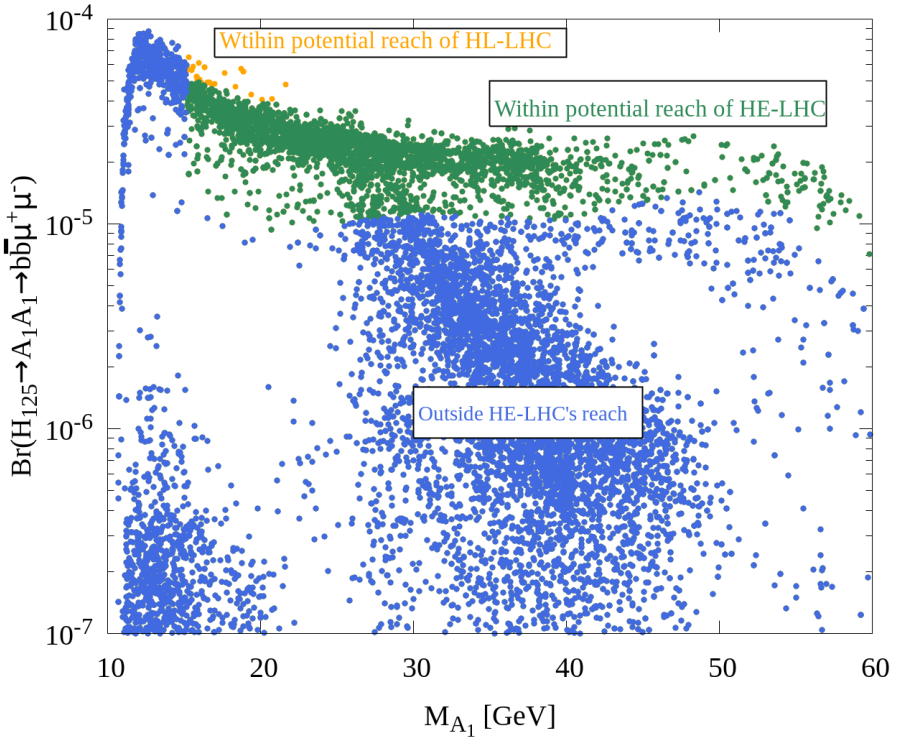

The future projections have been taken from *1902.00134 (Report from WG 2: Higgs Physics at the HL-LHC and HE-LHC, M. Cepeda et. al.) and translated to our allowed parameter space.*

- Blue colored points: Outside the projected reach.
- The results indicate that the discovery potential of light Higgs bosons produced via direct decays of H_{125} is not very strong.
- We made no attempt to optimize the analysis for increased luminosity or increased energy. So, our conclusion must be viewed with caution.

Projected reach of EW ino searches at the HL-LHC and HE-LHC

- We derive the projected reach at the HL-LHC and the HE-LHC for doublet higgsino production via the WZ and WH_{125} mediated $3l + \not{E}_{\rm T}$ channels through cut-based collider analyses using optimized signal regions.
- The projections are translated to the allowed NMSSM parameter space by considering the actual production cross-sections and branching ratios of the mixed states.
- In order to do so, we map out the efficiency grids in the doublet-higgsino LSP mass plane.

WZ-mediated $3l + \not{E}_{\mathrm{T}}$ at the HL-LHC

The following signal regions (SR) are used. We choose SRs optimized for large (BPB1, BPD1, BPG1), intermediate (BPE1, BPF1, BPH1) and small (BPA1, BPC1, BPF1) mass difference between NLSPs and the LSP.

	Benchmark points							
	BPA1	BPB1	BPC1	BPD1	BPE1	BPF1	BPG1	BPH1
$M_{\widetilde{\chi}_2^0,\widetilde{\chi}_3^0,\widetilde{\chi}_1^\pm}$ [GeV]	130	310	310	610	610	610	1000	1000
$M_{\widetilde{\chi}_1^0}$ [GeV]	30	0	210	0	300	510	0	420
Kinematic variables	Signal regions							
	SRA1	SRB1	SRC1	SRD1	SRE1	SRF1	SRG1	SRH1
$\Delta\Phi_{l_W \not{E}_{\mathrm{T}}}$	≤ 0.2	-	≤ 1.5	-	-	-	-	-
$\Delta\Phi_{SFOS-\not{E}_{\mathrm{T}}}$	-	$[2.7 : \pi]$	$[1.8 : \pi]$	$[1.5 : \pi]$	$[1.8 : \pi]$	-	$[1.6 : \pi]$	$[1.5 : \pi]$
ΔR_{SFOS}	$[1.4 : 3.8]$	$[0.3 : 2.1]$	-	$[0.1 : 1.3]$	$[0.1 : 1.3]$	$[1.6 : 4.0]$	$[0.1 : 1.0]$	$[0.1 : 1.3]$
$\not{E}_{\mathrm{T}}$ [GeV]	$[50 : 290]$	≥ 220	$[100 : 380]$	≥ 200	≥ 250	-	≥ 200	≥ 200
$M_T^{l_W}$ [GeV]	-	≥ 100	$[100 : 225]$	≥ 300	≥ 150	$[150 : 350]$	≥ 150	≥ 200
$M_{CT}^{l_W}$ [GeV]	-	≥ 100	-	≥ 100	≥ 150	$[100 : 400]$	≥ 200	≥ 200
$p_T^{l_1}$ [GeV]	$[50 : 150]$	≥ 120	$[60 : 110]$	≥ 150	≥ 150	$[60 : 150]$	≥ 210	≥ 200
$p_T^{l_2}$ [GeV]	$[50 : 110]$	≥ 60	≥ 30	≥ 100	≥ 100	$[50 : 80]$	≥ 150	≥ 100
$p_T^{l_3}$ [GeV]	≥ 30	≥ 30	≥ 30	≥ 50	≥ 50	$[30 : 60]$	≥ 50	≥ 50

Background generation (at LO) done using MadGraph5_aMC@NLO. Signal generated using Pythia-6 and detector effects simulated with Delphes-3.4.2.

WZ-mediated $3l + \not{E}_T$ at the HL-LHC

Projected reach of wino searches in the WZ mediated $3l + \not{E}_T$ final state at the HL-LHC.

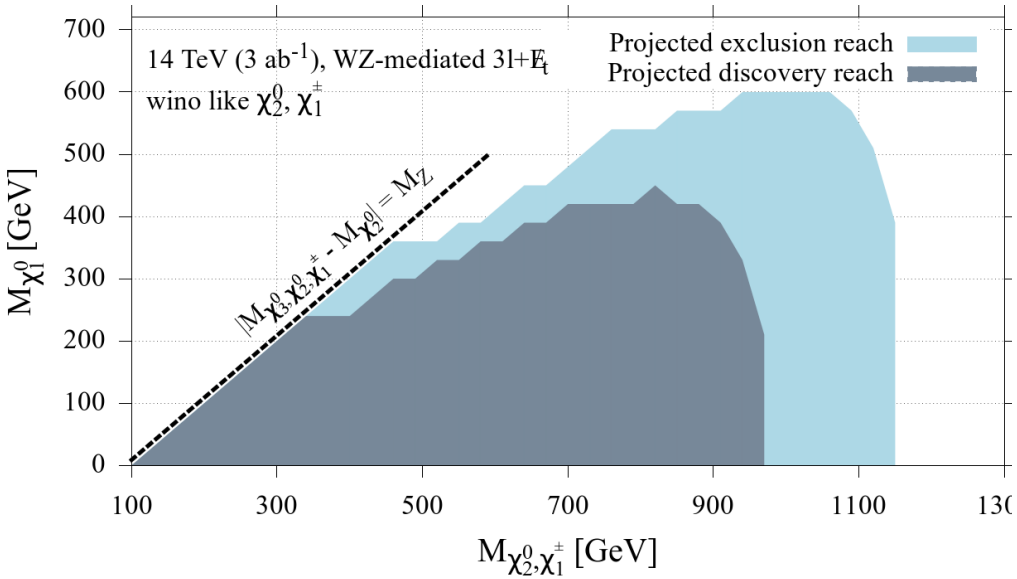

Our projection results are comparable with the ATLAS projections in ATL-PHYS-PUB-2018-048 (discovery (exclusion) upto $\sim$950 ($\sim$ 1110) GeV for massless LSP at 95% C.L.).

Efficiency maps:

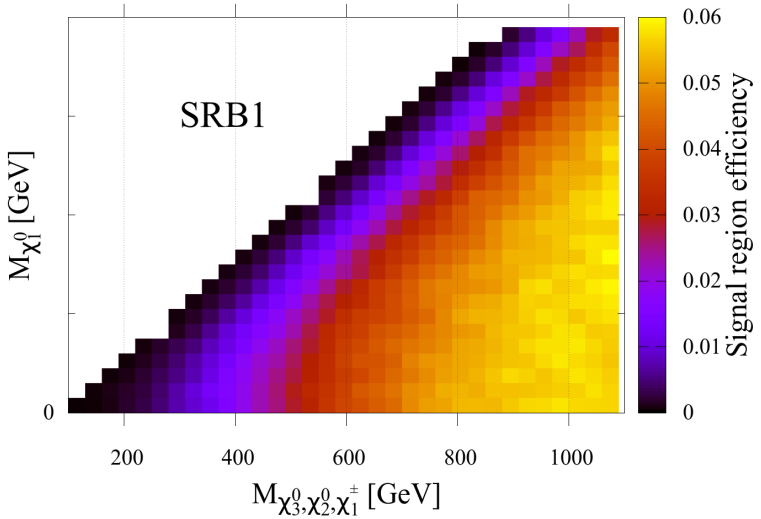

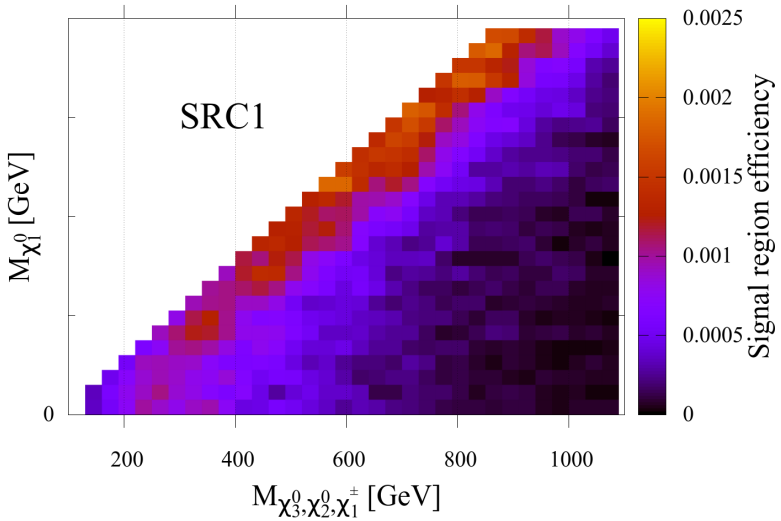

WZ-mediated $3l + \not{E}_T$ at the HL-LHC

Projected reach of wino searches in the WZ mediated $3l + \not{E}_T$ final state at the HL-LHC.

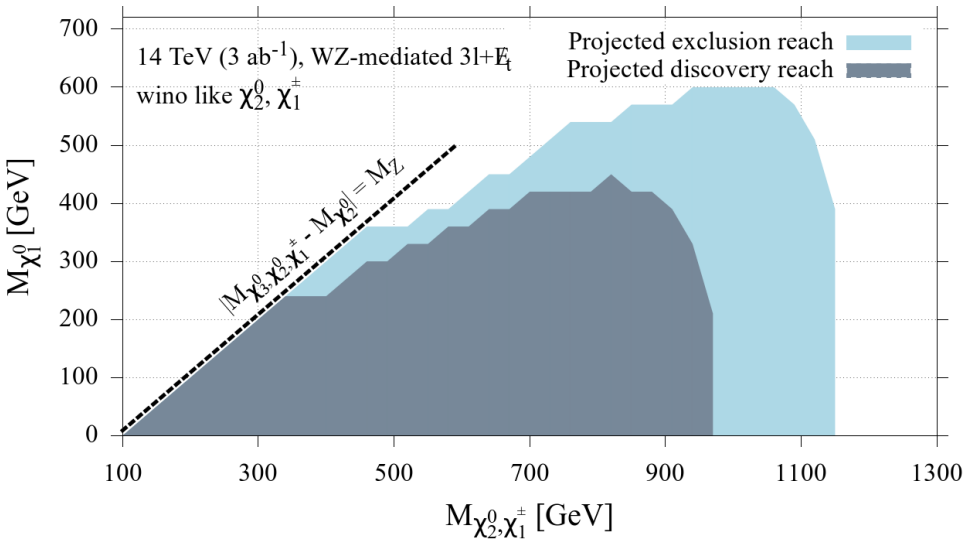

Our projection results are comparable with the ATLAS projections in ATL-PHYS-PUB-2018-048 (discovery (exclusion) upto $\sim$950 ($\sim$ 1110) GeV for massless LSP at 95% C.L.).

Projected reach of higgsino searches in the WZ mediated $3l + \not{E}_T$ final state at the HL-LHC.

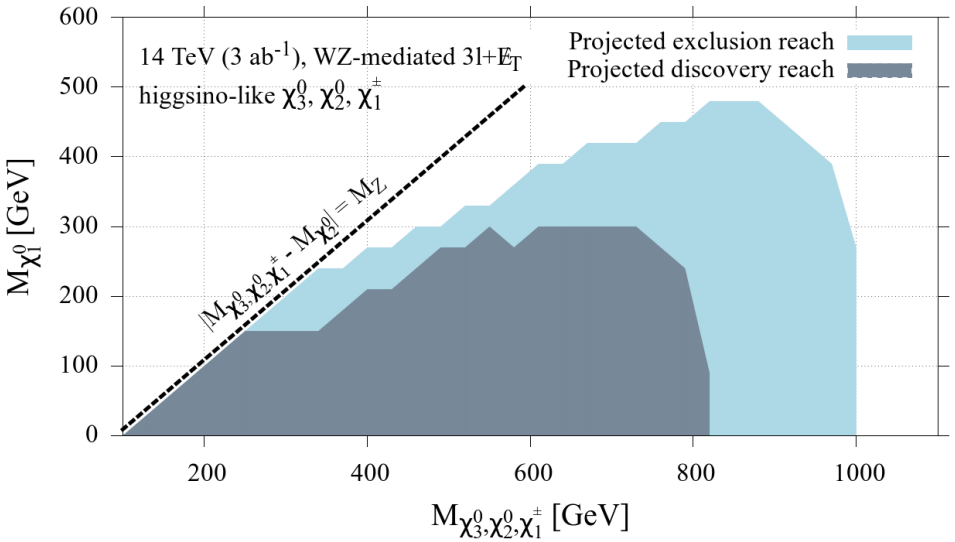

A systematic uncertainty of 5% has been assumed in these analyses.

Impact on allowed NMSSM parameter space

- In our allowed parameter region, $\widetilde{\chi}_2^0, \widetilde{\chi}_3^0, \widetilde{\chi}_4^0, \widetilde{\chi}_1^\pm, \widetilde{\chi}_2^\pm$ are either higgsino-like, wino-like or wino-higgsino admixtures.
- Direct chargino-neutralino pair production modes which can potentially contribute to WZ mediated $3l + \not{E}_{\mathrm{T}}$: $\widetilde{\chi}_2^0\widetilde{\chi}_1^\pm$, $\widetilde{\chi}_2^0\widetilde{\chi}_2^\pm$, $\widetilde{\chi}_3^0\widetilde{\chi}_1^\pm$, $\widetilde{\chi}_3^0\widetilde{\chi}_2^\pm$, $\widetilde{\chi}_4^0\widetilde{\chi}_1^\pm$ and $\widetilde{\chi}_4^0\widetilde{\chi}_2^\pm$
- The direct production cross-section ($\sigma_{\widetilde{\chi}_i^0\widetilde{\chi}_j^\pm}$) is computed by scaling the pure higgsino cross-section with the respective reduced squared $W\widetilde{\chi}_i^0\widetilde{\chi}_j^\pm$ couplings:

$$C^2_{W\widetilde{\chi}_i^0\widetilde{\chi}_j^\pm} = \left\{ \left(N_{i3}\ V_{j2} - N_{i2}\ V_{j1}\sqrt{2} \right)^2 + \left(N_{i4}\ U_{j2} + N_{i2}\ U_{j1}\sqrt{2} \right)^2 \right\}$$

U/V are the chargino mixing matrices while N represents the neutralino mixing matrix.

- The signal yield for a particular parameter space point is computed for all the signal regions through:

$$S = \sigma_{\widetilde{\chi}_i^0\widetilde{\chi}_j^\pm} \times (\textit{Relevant Br ratios}) \times (\mathcal{L} = 3000\ \mathrm{fb}^{-1}) \times \textit{Signal efficiency} \quad (1)$$

- The signal efficiency is obtained from the efficiency maps shown earlier.
- The signal significance (S_σ) is computed as: $S/\sqrt{B + (B \cdot sys\_un)^2}$, by adopting the signal region that yields the highest S_σ. Here, B stands for background.

Impact on allowed NMSSM parameter space

Color code: Green: $S_\sigma > 5$, light blue: $2 < S_\sigma < 5$, dark blue: $S_\sigma < 2$

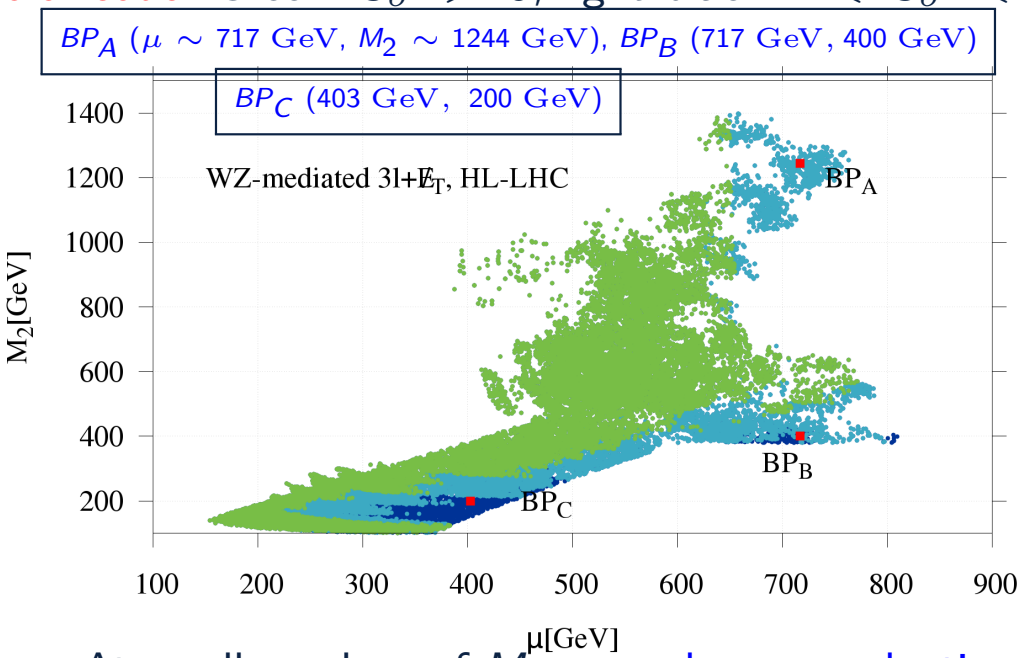

- The observation of a signal is an interplay between the production cross-section and signal efficiency.
- At large values of M_2, μ (near BP_A) $\rightarrow$ large efficiency but smaller production cross-section $\rightarrow$ kinematically suppressed signal.
- At smaller values of M_2, μ, $\rightarrow$ larger production cross-section but signal efficiencies reduce.
- The dark blue points near BP_C have S_σ marginally less than 2σ on account of smaller efficiency from SRB1 and suppressed $\widetilde{\chi}_2^0 \rightarrow Z\widetilde{\chi}_1^0$.
- In BP_B and BP_C, the dominant production mode is $\widetilde{\chi}_2^0\widetilde{\chi}_1^\pm$, and $\widetilde{\chi}_2^0$ dominantly decays into $H_{125} + \widetilde{\chi}_1^0$ with branching rates of 82% and 92%, respectively $\rightarrow$ reduced sensitivity in WZ mediated channels.
- Direct searches in WH_{125} mediated channels could be more effective for these benchmarks.

WH_{125}-mediated $3l + \not{E}_T$ at the HL-LHC

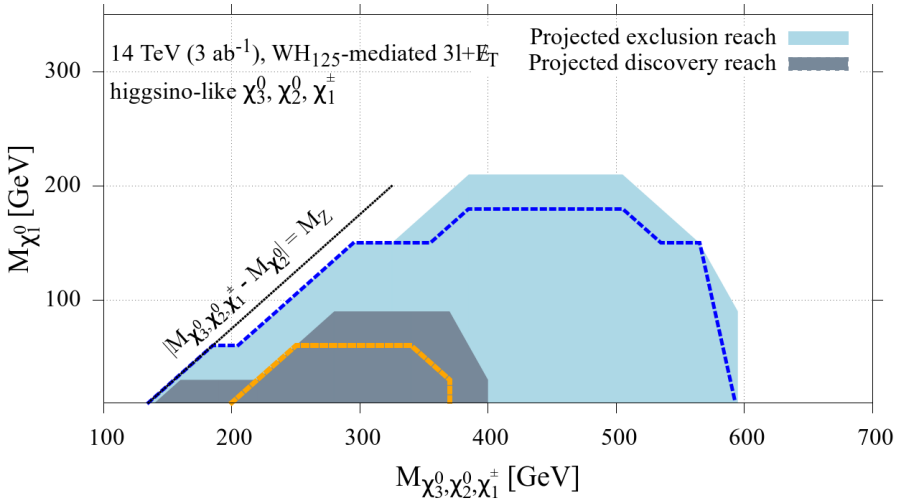

- Here, we use the optimized signal region cuts from ATL-PHYS-PUB-2014-010.

The figure at the bottom shows the projected reach on the currently allowed region $\rightarrow$ direct searches in the WH_{125} mediated $3l + \not{E}_T$ channel are more effective in probing the $M_2 \lesssim \mu$ region of parameter space.

- BP_B and BP_C: outside the reach of direct searches in WZ mediated $3l + \not{E}_T$, but fall within the discovery reach of direct searches in the WH_{125} mediated channel.
- Similarly, the $M_2 \lesssim 150$ GeV region in this figure shows 5σ sensitivity via the WZ mediated $3l + \not{E}_T$ search channel.
- We observe a striking complementarity in the search power via WZ and WH_{125} mediated $3l + \not{E}_T$ search channels..

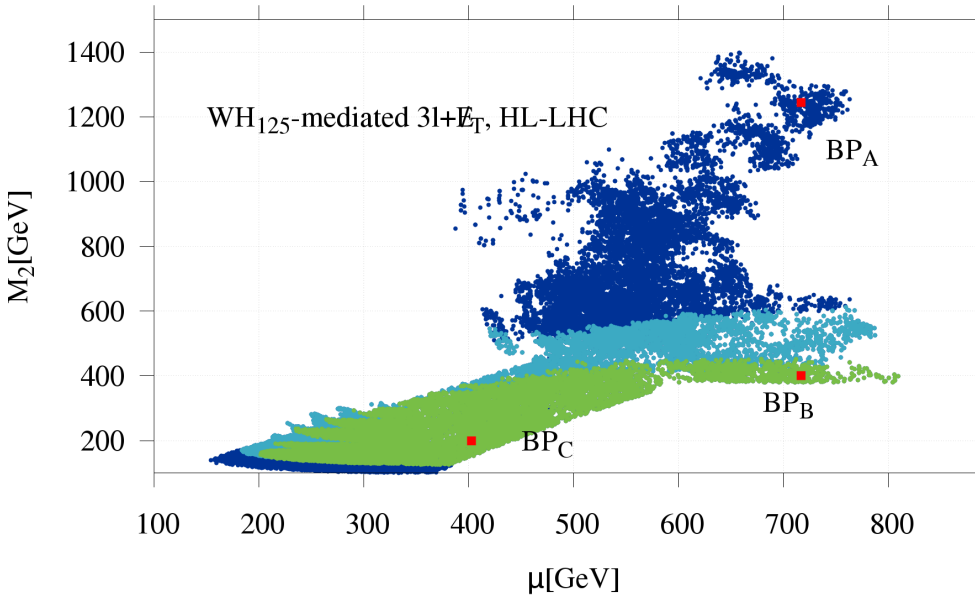

Scope of other complementary search channels in BP_B

	$\widetilde{\chi}_1^0$	$\widetilde{\chi}_2^0$	$\widetilde{\chi}_3^0$	$\widetilde{\chi}_4^0$	$\widetilde{\chi}_1^\pm$	$\widetilde{\chi}_2^\pm$
Mass [GeV]	60.4	421	734	742	421	741
wino %	10^{-5}	0.96	2×10^{-3}	0.04	0.94	0.06
higgsino %	10^{-4}	0.04	0.99	0.96	0.06	0.94

Singlino fraction in $\widetilde{\chi}_1^0$: 0.99			$M_{H_1} = 97.2$ GeV, $M_{A_1} = 99$ GeV			
Cross-section (fb)	$\widetilde{\chi}_2^0\widetilde{\chi}_1^\pm$	$\widetilde{\chi}_2^0\widetilde{\chi}_2^\pm$	$\widetilde{\chi}_3^0\widetilde{\chi}_1^\pm$	$\widetilde{\chi}_3^0\widetilde{\chi}_2^\pm$	$\widetilde{\chi}_4^0\widetilde{\chi}_1^\pm$	$\widetilde{\chi}_4^0\widetilde{\chi}_2^\pm$
$\sqrt{s} = 14$ TeV	104	0.27	0.28	2.1	0.25	2.3
$\sqrt{s} = 27$ TeV	363	1.1	1.1	10.2	1.0	11.2
Branching ratio	$\widetilde{\chi}_2^0 \to \widetilde{\chi}_1^0 Z$ (0.04), $\widetilde{\chi}_1^0 H_{125}$ (0.82), $\widetilde{\chi}_1^0 H_1$ (0.14)					
	$\widetilde{\chi}_3^0 \to \widetilde{\chi}_1^0 Z$ (0.13), $\widetilde{\chi}_1^0 H_{125}$ (0.10), $\widetilde{\chi}_1^0 H_1$ (0.01), $\widetilde{\chi}_1^\pm W^\mp$ (0.51), $\widetilde{\chi}_2^0 Z$ (0.23), $\widetilde{\chi}_2^0 H_{125}$ (0.01)					
	$\widetilde{\chi}_4^0 \to \widetilde{\chi}_1^0 Z$ (0.12), $\widetilde{\chi}_1^0 H_{125}$ (0.11), $\widetilde{\chi}_1^\pm W^\mp$ (0.53) $\widetilde{\chi}_4^0 \to \widetilde{\chi}_2^0 Z$ (0.02), $\widetilde{\chi}_2^0 H_{125}$ (0.21)					
Significance at HL-LHC: WZ mediated $3l + \not{E}_{\rm T}$: 1.5, WH_{125} mediated $3l + \not{E}_{\rm T}$: 5.3 Significance at HE-LHC: WZ mediated $3l + \not{E}_{\rm T}$: 4.4, WH_{125} mediated $3l + \not{E}_{\rm T}$: 34						

- Notice the presence of other cascade decay modes:
  1. $\widetilde{\chi}_3^0$ can decay into $\widetilde{\chi}_2^0 Z$, while $\widetilde{\chi}_2^0$ can decay into $\widetilde{\chi}_1^0 H_1$ or $\widetilde{\chi}_1^0 H_{125}$.
  2. $\widetilde{\chi}_3^0$ is dominantly produced in association with $\widetilde{\chi}_2^\pm$, which can decay into $Z/H_{125} + \widetilde{\chi}_1^\pm$ or $W^\pm + \widetilde{\chi}_2^0/\widetilde{\chi}_1^0$ with appreciable rates.
  3. $\widetilde{\chi}_3^0\widetilde{\chi}_2^\pm$ can eventually lead to rich final states including $VV + \not{E}_{\rm T}$ or $V/Z/H_1 + \not{E}_{\rm T}$. Although, $\sigma(\widetilde{\chi}_3^0\widetilde{\chi}_2^\pm)$ is small for BP_B, but one obtain points with relatively larger $\sigma(\widetilde{\chi}_3^0\widetilde{\chi}_2^\pm)$, for. eg. BP_C with $\sigma(\widetilde{\chi}_3^0\widetilde{\chi}_2^\pm) \sim 24.8$ fb.
- $3l + \not{E}_{\rm T}$ channels might not be most the efficient ones in the presence of these cascade decay channels.
- Dedicated searches beyond the scope of this work will be needed to explore these novel signals.

Projected reach of doublet higgsino searches at the HE-LHC

Color code: Grey: projected discovery region, light blue: projected exclusion region

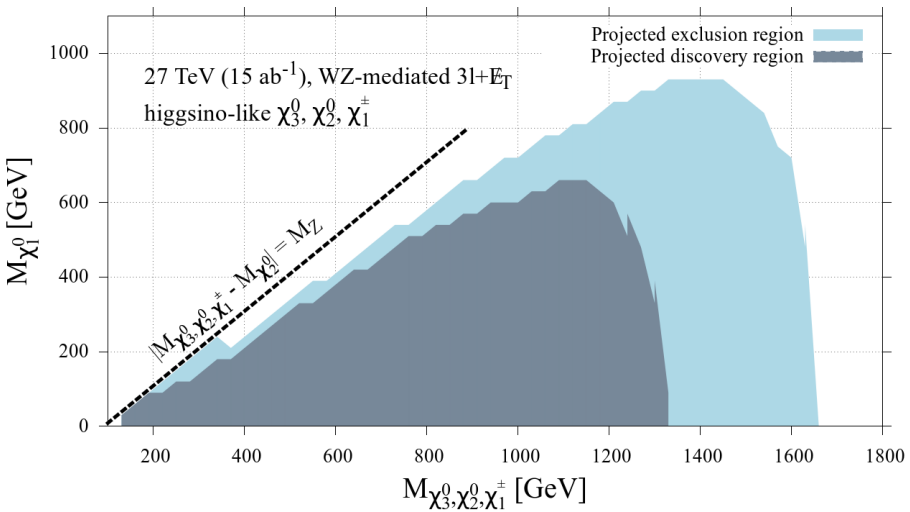

- We optimize 7 different signal regions to perform this search.
- Projected exclusion reach at the HL-LHC was only up to ~ 600 GeV.

- We perform our own collider analysis and 10 optimized signal regions are considered.
- Considerable improvement over its HL-LHC counterpart. Projected exclusion reach at the HL-LHC was only up to ~ 1000 GeV for massless $\widetilde{\chi}_1^0$.

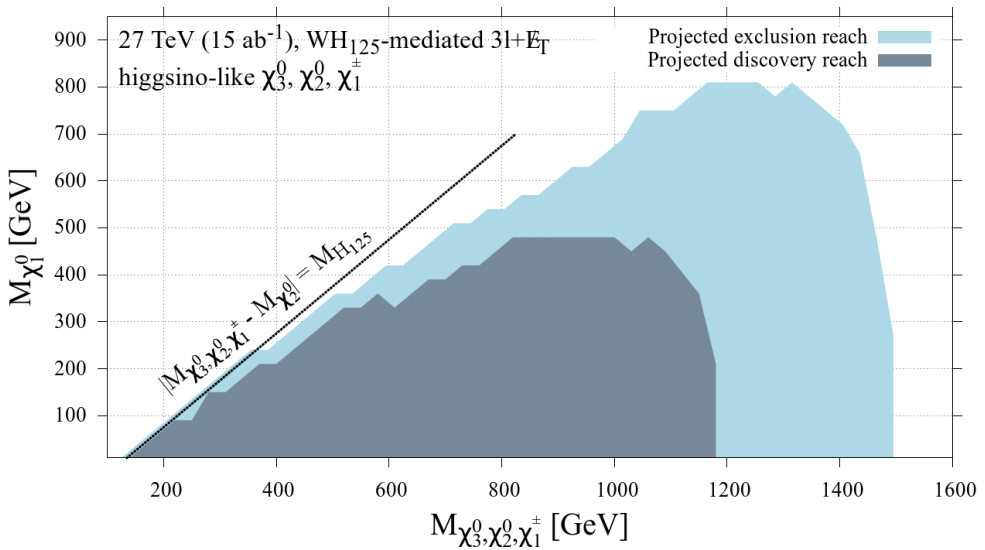

Color code: Green: $S_\sigma > 5$, light blue: $2 < S_\sigma < 5$, dark blue: $S_\sigma < 2$

WZ-mediated $3l + \not{E}_T$ channel

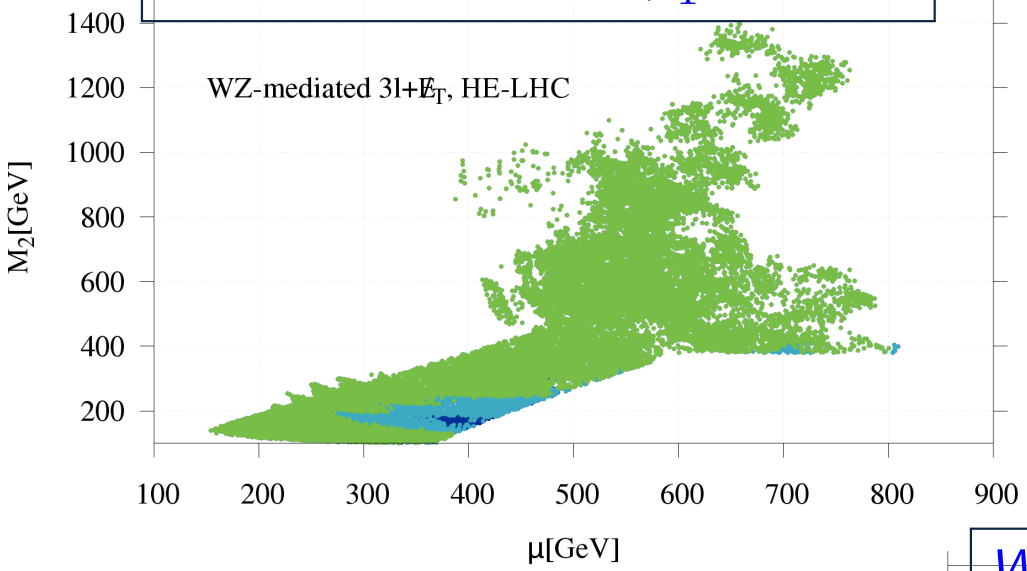

The HE-LHC provides a larger discovery opportunity than the HL-LHC for the detection of NMSSM inos with light LSP.

WH_{125}-mediated $3l + \not{E}_T$ channel

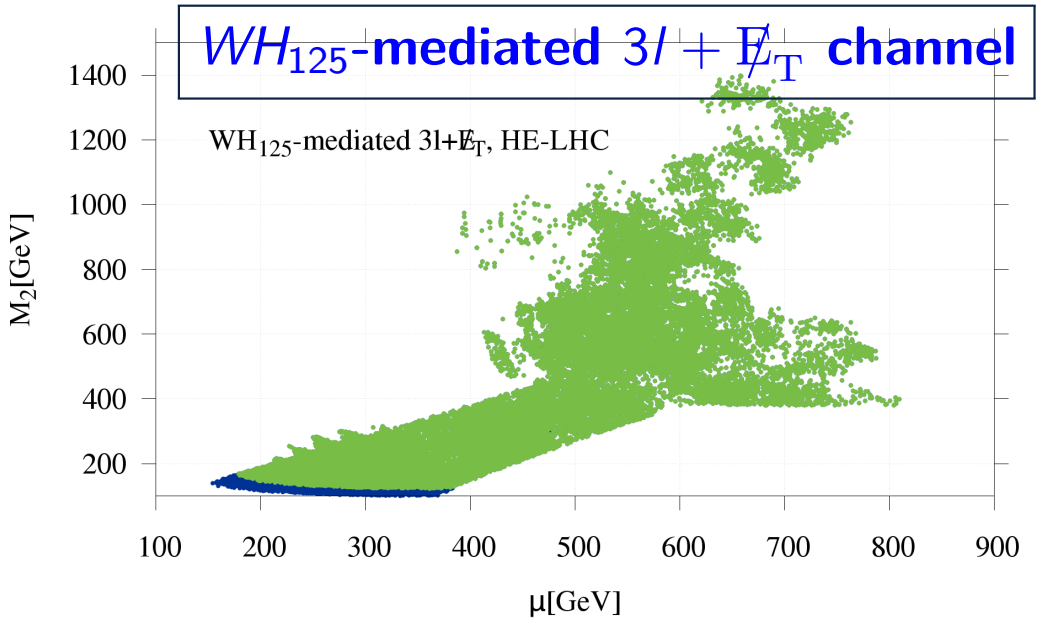

Combination of EW ino searches in the WZ and WH_{125} mediated $3l + \not{E}_T$ channel will probe all the currently allowed parameter space points at discovery potential.

Future directions

Light Higgs phenomenology

- Benchmark studies focused on exploring the parameter region with light H_1/A_1 at the future high-energy colliders through dedicated searches in various final states, viz. the 4τ final state.
- Study of complementarity between the direct light Higgs search projections and the invisible Higgs width measurement capability of the linear colliders.

The alternate probes for electroweakino searches

- Benchmark points BP_B and BP_C indicated towards the possibility of having cascade decays which culminate in final states which are different from the traditional search channels.
- These novel search modes might provide complementary probes for benchmark points with cascade decays and could increase the discovery reach at the future colliders.

A comprehensive study of the light singlino region of parameter space

- We find light singlino-like LSPs with mass as small as $\sim$1 GeV compatible with the current collider, astrophysical and cosmological constraints.
- Despite having a pseudoscalar Higgs as the mediator, the annihilation cross-section of these light singlinos is found to be small enough to avoid any implications from the current indirect constraints while also generating an under-abundant relic.
- This sector would require a more careful study.

Thank you

Backup slides

Benchmark points

Benchmark points	Input parameters
BP_A	$\lambda = 0.3$, $\kappa = 0.01$, $\tan\beta = 9.5$, $A_\lambda = 6687$ GeV, $A_\kappa = 5.2$ GeV, $\mu = 717$ GeV, $M_2 = 1244$ GeV, $M_3 = 2301$ GeV
BP_B	$\lambda = 0.44$, $\kappa = 0.02$, $\tan\beta = 11.8$, $A_\lambda = 8894$ GeV, $A_\kappa =$ -57 GeV, $\mu = 717$ GeV, $M_2 = 400$ GeV, $M_3 = 4323$ GeV
BP_C	$\lambda = 0.08$, $\kappa = 3 \times 10^{-4}$, $\tan\beta = 18$, $A_\lambda = 6563$ GeV, $A_\kappa =$ -7.9 GeV, $\mu = 403$ GeV, $M_2 = 200$ GeV $M_3 = 3080$ GeV
BP_D	$\lambda = 0.44$, $\kappa = 0.02$, $\tan\beta = 15.6$, $A_\lambda = 585$ GeV, $A_\kappa = 9501$ GeV, $\mu = 585$ GeV, $M_2 = 952$ GeV, $M_3 = 4457$ GeV
BP_E	$\lambda = 0.27$, $\kappa = 0.02$, $\tan\beta = 11.6$, $A_\lambda = 5875$ GeV, $A_\kappa = 12$ GeV, $\mu = 518$ GeV, $M_2 = 696$ GeV, $M_3 = 3634$ GeV
BP_F	$\lambda = 0.30$, $\kappa = 0.01$, $\tan\beta = 11.2$, $A_\lambda = 6319$ GeV, $A_\kappa = 17$ GeV, $\mu = 571$ GeV, $M_2 = 555$ GeV, $M_3 = 2687$ GeV
BP_G	$\lambda = 0.42$, $\kappa = 0.02$, $\tan\beta = 15.9$, $A_\lambda = 8638$ GeV, $A_\kappa = 43.4$ GeV, $\mu = 515$ GeV, $M_2 = 396$ GeV, $M_3 = 2903$ GeV
BP_H	$\lambda = 0.02$, $\kappa = 7 \times 10^{-5}$, $\tan\beta = 25.5$, $A_\lambda = 7348$ GeV, $A_\kappa =$ -7.3 GeV, $\mu = 302$ GeV, $M_2 = 204$ GeV, $M_3 = 2239$ GeV
BP_I	$\lambda = 0.02$, $\kappa = 6 \times 10^{-5}$, $\tan\beta = 27.6$, $A_\lambda = 6924$ GeV, $A_\kappa =$ -5.7 GeV, $\mu = 262$ GeV, $M_2 = 210$ GeV, $M_3 = 2217$ GeV

1. Why NMSSM?
2. Outline of this work
3. Prospects at future DD experiments and e^+-e^- colliders
4. Projected reach of electroweakino searches at the HL-LHC and HE-LHC
5. Implications from current constraints

The allowed parameter space

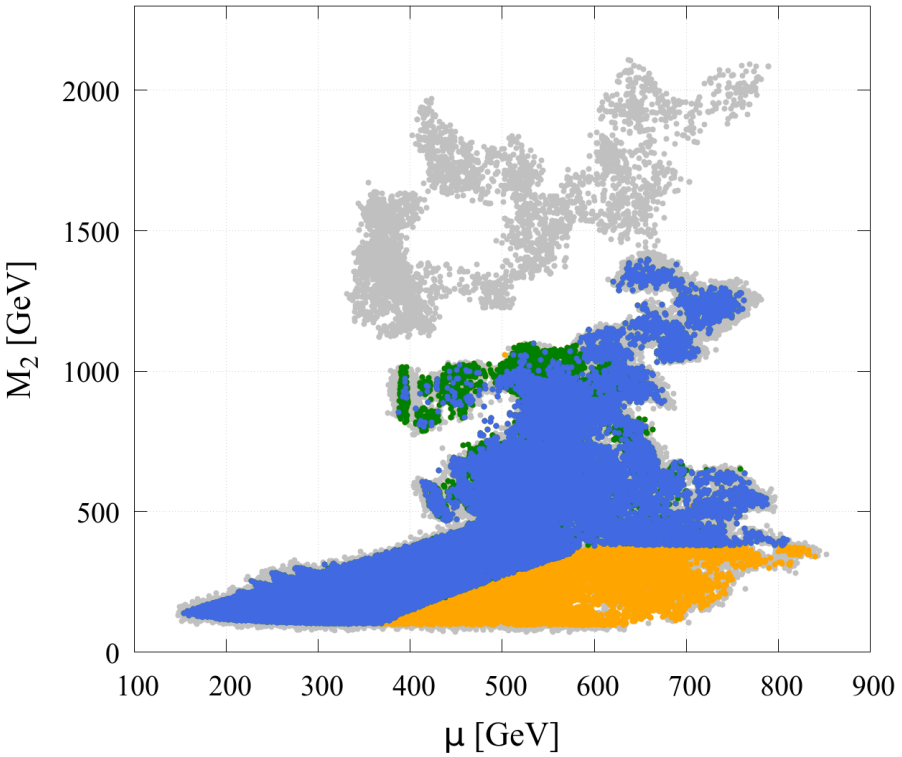

- Blue color: The allowed parameter space points.
- The grey and green points also lie beneath the blue and yellow colored points.

- Grey points: excluded by the constraints from: LEP, Higgs signal strength, B physics, direct light Higgs searches and sparticle searches at the LHC.
- Green and yellow regions: excluded by the SI direct detection limits from Xe-1T and the limits from direct EW ino searches in the $3l + \not{E}_{\mathrm{T}}$ and $2l + \not{E}_{\mathrm{T}}$ channels, respectively.
- The points in the large M_2 region are mostly excluded by the Higgs signal strength constraints, requirement of a 125 GeV Higgs and LEP searches for light Higgs.

Event yields at the HL-LHC and the HE-LHC

We see a considerable improvement in the signal yields at the high energy upgrade of the LHC.

Benchmark point	WZ mediated		WH_{125} mediated	
(M_2, μ) [in GeV]	HL-LHC	HE-LHC	HL-LHC	HE-LHC
BP_A	13	180	4	23
(1244, 717)	(3.8)	(14)	(0.4)	(6.6)
BP_B	7	86	63	272
(400, 717)	(1.5)	(4.4)	(5.3)	(34)
BP_C	7	65	131	388
(200, 403)	(1.3)	(2.1)	(8.8)	(48)
BP_D	20	231	8	35
(952, 585)	(6.1)	(18)	(1.0)	(9.8)
BP_E	23	408	12	36
(696, 518)	(7.0)	(20)	(1.2)	(10)
BP_F	28	418	18	79
(555, 571)	(8.6)	(21)	(2.1)	(22)
BP_G	23	233	78	206
(396, 515)	(5.2)	(12)	(5.3)	(27)
BP_H	17	167	125	368
(204, 302)	(3.4)	(5.3)	(8.4)	(45)
BP_I	27	257	110	321
(210, 262)	(5.3)	(8.1)	(7.4)	(40)

The numbers in represents the signal significance values.

References I

D. Albornoz Vasquez, G. Belanger, and C. Boehm.

Astrophysical limits on light NMSSM neutralinos.
Phys. Rev., D84:095008, 2011.

D. Albornoz Vasquez, G. Belanger, C. Boehm, A. Pukhov, and J. Silk.

Can neutralinos in the MSSM and NMSSM scenarios still be light?
Phys. Rev., D82:115027, 2010.

D. Barducci, G. Belanger, C. Hugonie, and A. Pukhov.

Status and prospects of the nMSSM after LHC Run-1.
JHEP, 01:050, 2016.

R. K. Barman, G. Belanger, B. Bhattacherjee, R. Godbole, G. Mendiratta, and D. Sengupta.

Invisible decay of the Higgs boson in the context of a thermal and nonthermal relic in MSSM.
Phys. Rev., D95(9):095018, 2017.

G. Belanger, F. Boudjema, A. Cottrant, A. Pukhov, and S. Rosier-Lees.

Lower limit on the neutralino mass in the general MSSM.
JHEP, 03:012, 2004.

G. Belanger, F. Boudjema, C. Hugonie, A. Pukhov, and A. Semenov.

Relic density of dark matter in the NMSSM.
JCAP, 0509:001, 2005.

G. Belanger, G. Drieu La Rochelle, B. Dumont, R. M. Godbole, S. Kraml, and S. Kulkarni.

LHC constraints on light neutralino dark matter in the MSSM.
Phys. Lett., B726:773–780, 2013.

C. Boehm, P. S. B. Dev, A. Mazumdar, and E. Pukartas.

Naturalness of Light Neutralino Dark Matter in pMSSM after LHC, XENON100 and Planck Data.
JHEP, 06:113, 2013.

References II

L. Calibbi, T. Ota, and Y. Takanishi.

Light Neutralino in the MSSM: a playground for dark matter, flavor physics and collider experiments.
JHEP, 07:013, 2011.

J.-J. Cao, K.-i. Hikasa, W. Wang, J. M. Yang, K.-i. Hikasa, W.-Y. Wang, and J. M. Yang.

Light dark matter in NMSSM and implication on Higgs phenomenology.
Phys. Lett., B703:292–297, 2011.

D. G. Cerdeno, P. Ghosh, and C. B. Park.

Probing the two light Higgs scenario in the NMSSM with a low-mass pseudoscalar.
JHEP, 06:031, 2013.

F. Domingo, U. Ellwanger, E. Fullana, C. Hugonie, and M.-A. Sanchis-Lozano.

Radiative Upsilon decays and a light pseudoscalar Higgs in the NMSSM.
JHEP, 01:061, 2009.

U. Ellwanger and C. Hugonie.

The semi-constrained NMSSM satisfying bounds from the LHC, LUX and Planck.
JHEP, 08:046, 2014.

U. Ellwanger and C. Hugonie.

The higgsinoâĂŞsinglino sector of the NMSSM: combined constraints from dark matter and the LHC.
Eur. Phys. J., C78(9):735, 2018.

D. Feldman, Z. Liu, and P. Nath.

Low Mass Neutralino Dark Matter in the MSSM with Constraints from $B_s \to \mu^+ \mu^-$ and Higgs Search Limits.
Phys. Rev., D81:117701, 2010.

M. Guchait and A. Roy.

Light Singlino Dark Matter at the LHC.
5 2020.

References III

K. Hamaguchi and K. Ishikawa.

Prospects for Higgs- and Z-resonant Neutralino Dark Matter.
Phys. Rev., D93(5):055009, 2016.

D. Hooper and T. Plehn.

Supersymmetric dark matter: How light can the LSP be?
Phys. Lett., B562:18–27, 2003.

J. Kozaczuk and S. Profumo.

Light NMSSM neutralino dark matter in the wake of CDMS II and a 126 GeV Higgs boson.
Phys. Rev., D89(9):095012, 2014.

F. Mahmoudi, J. Rathsman, O. Stal, and L. Zeune.

Light Higgs bosons in phenomenological NMSSM.
Eur. Phys. J., C71:1608, 2011.

A. M. Sirunyan et al.

Search for an exotic decay of the Higgs boson to a pair of light pseudoscalars in the final state of two muons and two τ leptons in proton-proton collisions at $\sqrt{s} = 13$ TeV.
JHEP, 11:018, 2018.

A. M. Sirunyan et al.

Search for an exotic decay of the Higgs boson to a pair of light pseudoscalars in the final state with two b quarks and two τ leptons in proton-proton collisions at $\sqrt{s} = 13$ TeV.
Phys. Lett., B785:462, 2018.

K. Wang and J. Zhu.

Funnel annihilations of light dark matter and the invisible decay of the Higgs boson.
Phys. Rev. D, 101:095028, 2020.